Novel Mechanism of a Charge Density Wave in a Transition Metal Dichalcogenide

D. W. Shen,[1] B. P. Xie,[1] J. F. Zhao,[1] L. X. Yang,[1] L. Fang,[2] J. Shi,[3] R. H. He,[4] D. H. Lu,[4] H. H. Wen,[2] and D. L. Feng[1,*]

[1]*Department of Physics, Applied Surface Physics State Key Laboratory, Fudan University, Shanghai 200433, China*

[2]*National Lab for Superconductivity, Institute of Physics and National Lab for Condensed Matter Physics, Chinese Academy of Sciences, P.O. Box 603, Beijing 100080, People's Republic of China*

[3]*School of Physics, Wuhan University, Wuhan, 430072, People's Republic of China*

[4]*Department of Applied Physics and Stanford Synchrotron Radiation Laboratory, Stanford University, Stanford, California 94305, USA*

(Received 22 November 2006; published 21 November 2007)

The charge density wave (CDW) is usually associated with Fermi surfaces nesting. We here report a new CDW mechanism discovered in a 2*H*-structured transition metal dichalcogenide, where the two essential ingredients of the CDW are realized in very anomalous ways due to the strong-coupling nature of the electronic structure. Namely, the CDW gap is only partially open, and charge density wave vector match is fulfilled through participation of states of the large Fermi patch, while the straight Fermi surface sections have secondary or negligible contributions.

DOI: 10.1103/PhysRevLett.99.216404 PACS numbers: 71.18.+y, 71.45.Lr, 79.60.−i

It has been a standard textbook example that the charge density wave (CDW), one of the main forms of ordering in solid, is mostly associated with nesting Fermi surface (FS) sections. In charge ordered materials ranging from one-dimensional (1D) $(TaSe_4)_2I$ and blue bronze [1,2] to two-dimensional (2D) manganites, and from surface reconstruction in weak correlated metals to the checkerboard pattern of strongly correlated high temperature superconductors [3,4], the charge fluctuations associated with the ordering wave vector scatter the electrons between two nested FS sections and effectively drive the system into an ordered ground state. However, this classical picture failed in the very first 2D CDW compound discovered in 1974, i.e., the transition metal dichalcogenides (TMD's) [5]. The 2*H*-structured TMD's have a hexagonal lattice structure, and in its CDW phase, a 3×3 superlattice forms [5,6]. It was found that the ordering wave vectors do not match the nested FS sections, and generally no CDW energy gap was observed at the FS [7,8]. After decades of continuous effort and invalidation of the conventional mechanisms, it is extremely enigmatic why CDW could occur in 2*H*-TMD systems. Subsequently, the competition and coexistence of CDW and superconductivity in TMD's [9] remain to be revealed [10].

In this Letter, we studied the electronic origin of the CDW in a 2*H*-TMD, 2*H*-Na_xTaS_2, by angle-resolved photoemission spectroscopy (ARPES). The CDW mechanism in this material was discovered after the revelation of the following exotic properties. (i) The electronic structure exhibits a strong-coupling nature, with finite density of states at the Fermi energy (E_F) over almost the entire Brillouin zone (BZ), forming so-called Fermi patches. (ii) In the CDW state, only a fraction of the states at E_F is gapped. (iii) The density of states near E_F directly correlates with the ordering strength. (iv) Fermi patch, instead of Fermi surface, is relevant for CDW. We show that this new "Fermi-patch mechanism" for CDW is rooted in the strong-coupling nature of the electronic structure and it may be a general theme of ordering in the strong-coupling regime of various models, and applicable to systems with a similar electronic structure.

For the systematic studies of the electronic structure in a 2*H*-TMD compound, 2*H*-Na_xTaS_2 with 2%, 5%, and 10% Na concentration were synthesized with CDW transition temperature T_{CDW}'s at 68 K, 65 K, and 0 K, respectively [11]. The samples are labeled as $CDW^{68\ K}$, $CDW^{65\ K}$, and $CDW^{0\ K}$ hereafter. The corresponding superconducting transition temperatures are 1.0 K, 2.3 K, and 4.0 K, respectively, a manifestation of the competition between CDW and superconductivity in this system. The data were mainly collected using the 21.2 eV Helium-I line of a discharge lamp combined with a Scienta R4000 analyzer, and partial measurements were carried out on beam line 5-4 of Stanford Synchrotron Radiation Laboratory (SSRL). The overall energy resolution is 8 meV, and the angular resolution is 0.3°.

Photoemission spectra taken on samples with ($CDW^{65\ K}$) and without CDW ($CDW^{0\ K}$) are compared in Figs. 1(a)–1(d). In both cases, the spectral line shapes are remarkably broad, and no quasiparticle peaks in the conventional sense are observed. The large linewidth is of the same order as the dispersion, which clearly indicates the incoherent nature of the spectrum, and the system is in the *strong-coupling* regime. Taking the normalized spectra at **M** as Ref. [12], spectra at Γ, **K**, and the Fermi crossing of the Γ-**M** cut are compared in Fig. 1(e). The difference between $CDW^{0\ K}$ and $CDW^{65\ K}$ is striking. Although they have similar density of states at the Fermi crossing area, for momentum regions away from the FS, $CDW^{65\ K}$ has a much stronger spectral weight than $CDW^{0\ K}$, no matter whether it is inside the occupied region (**M** point) or in the unoccupied region (Γ and **K** points) in the band structure calculations [13]. Particularly, one finds that even when the spectral centroid is well below E_F, the finite residual

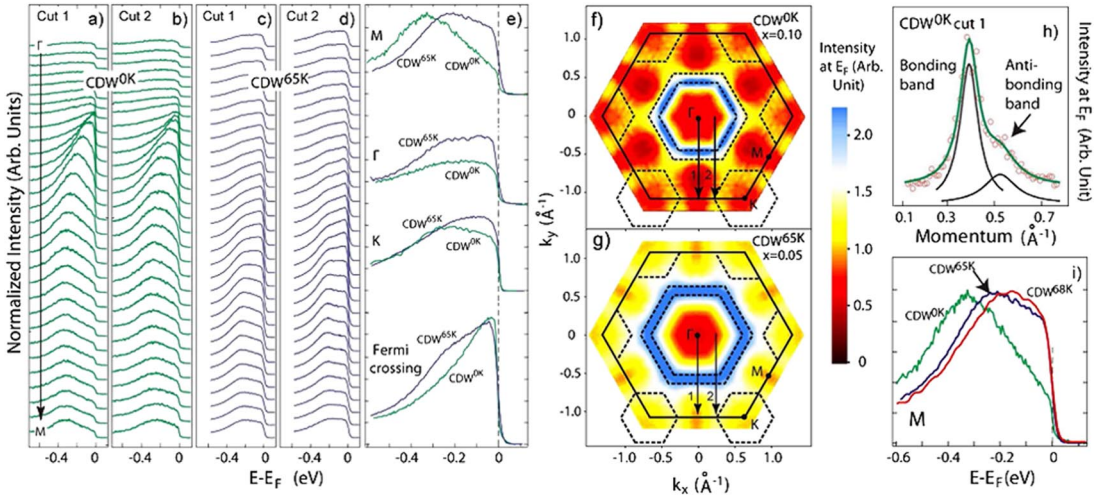

FIG. 1 (color online). Typical ARPES spectra for (a),(b) $CDW^{0\ K}$ at $T = 15$ K and (c),(d) $CDW^{65\ K}$ at $T = 95$ K, respectively, at equal angle spacing along the marked cuts in the Brillouin zone in (f),(g). (e) Comparison of photoemission spectra for different $2H$-Na_xTaS_2's at high symmetry points **M** [also in (i)], Γ, **K**, and at the Fermi crossing of cut 1. (f),(g) The photoemission intensity integrated within 10 meV of E_F is shown for $CDW^{0\ K}$ and $CDW^{65\ K}$, respectively. (Both data were taken at 15 K and the image was sixfold symmetrized.) The Fermi surfaces are marked by dashed lines, where the antibonding and bonding bands could be resolved for the Γ pockets in the momentum distribution curve [one example is shown in (h) for $CDW^{0\ K}$].

weight at E_F beyond background exists around **M**. We note that the $CDW^{0\ K}$ sample has higher Na doping than $CDW^{65\ K}$, yet its line shape is generally sharper. Therefore, disorder effects induced by the dopants should be negligible. The residual weight observed near E_F thus should be associated with the intrinsic strong-coupling nature of the system, which (within several $k_B T_{CDW}$ around E_F) shows a monotonic correlation with T_{CDW} in Fig. 1(i).

The wide spread of the large spectral weight at E_F for $CDW^{65\ K}$ (in comparison with $CDW^{0\ K}$) is clearly illustrated in Figs. 1(f) and 1(g), where almost the entire BZ of $CDW^{65\ K}$ appears to be one gigantic Fermi patch. On the other hand, Fermi surfaces could still be defined as the contour of the local maxima (dashed lines) [14]. Three FS pockets can be identified through the momentum distribution curve analysis: two hole pockets around Γ, as exemplified in Fig. 1(h), and one hole pocket around **K**. Bilayer band splitting of the two TaS_2 layers in a unit cell manifests itself as the inner and outer Gamma pockets, while the splitting of the **K** pockets is indistinguishable. The FS volumes are evaluated to be 1.05 ± 0.01 and 1.11 ± 0.01 electrons per layer for the 5% and 10% Na doped Na_xTaS_2 samples, respectively, consistent with the nominal dopant concentrations. This resembles the high temperature superconductors, where the Fermi surfaces defined in this conventional way are consistent with the band structure calculations and follow the Luttinger sum rule quite well [15], yet there are large Fermi patches near the antinodal regions [16].

Searches for the CDW mechanism were mostly focused on the Fermi surfaces of the $2H$-TMD's before. Intrigued by the differences between $CDW^{65\ K}$ and $CDW^{0\ K}$ spectra in the Fermi-patch region [Fig. 1(e)], Figs. 2(a) and 2(b) examine spectra taken from **M** at different temperatures for $CDW^{65\ K}$ and $CDW^{0\ K}$, respectively. While the $CDW^{0\ K}$ spectra simply exhibit a clear Fermi crossing and thermal broadening, the $CDW^{65\ K}$ spectra appear very anomalous. Take the spectrum at 7 K as an example; while the upper part of the spectrum is suppressed to higher binding energies, the middle point of the leading edge of the lower part still matches E_F. There is an apparent turning point between these two parts of the spectrum. By dividing the spectra with the corresponding finite temperature Fermi-Dirac distribution functions, in Fig. 2(c), one clearly observes that about 29% of the spectral weight at E_F has been suppressed for $CDW^{65\ K}$. An energy gap has opened on part of the states here, which is estimated to be

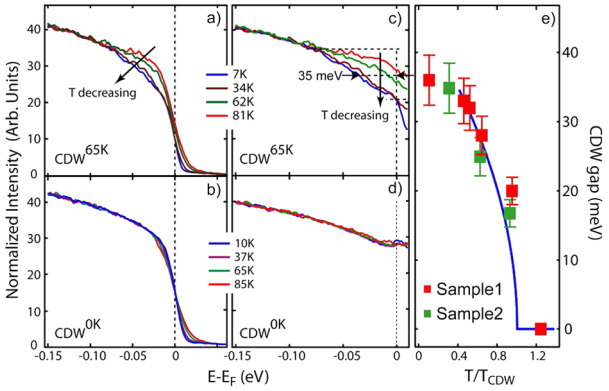

FIG. 2 (color online). The CDW gap measurements of $2H$-Na_xTaS_2. ARPES spectra taken at **M** for different temperatures for (a) $CDW^{65\ K}$ and (b) $CDW^{0\ K}$. (c),(d) The spectra in (a),(b) divided by the resolution convoluted Fermi-Dirac distribution at the corresponding temperatures. (e) The temperature dependence of the CDW gap. The solid line is the fit to a mean field formula, $\Delta_0\sqrt{1-(T/T_{CDW})}$.

~35 meV based on the middle point of the leading edge [17]. Contrastively, there is no sign of gap opening for CDW$^{0\ K}$ [Fig. 2(d)]. The temperature evolution of the gap is shown in Fig. 2(e) for two different CDW$^{65\ K}$ samples, which can be described well by the mean field formula $\Delta_0\sqrt{1-(T/T_{CDW})}$ near T_{CDW} [18]. The partial gap might be related to the recent suggestion that a $2H$-TMD system is decoupled into three sublattices: one being undistorted and gapless below T_{CDW}, the other two being gapped at the FS [19]. However, we note that a partial gap here does not occur at the FS, and with less weight being gapped.

Both temperature dependence and the doping dependence of the observed partial gap have unambiguously illustrated its CDW origin. Taking the above conventional definition [17], the CDW gap was mapped over the entire Brillouin zone for CDW$^{65\ K}$ [upper half of Fig. 3(a)]. Strikingly, a finite CDW gap exists over most of the Brillouin zone. Its maximum locates around **M**, and no gap is observed around the inner Γ Fermi pocket and within. Noticeably, the gap is finite in the **K** Fermi pockets, as there is finite spectral weight at E_F. Close comparisons of spectra at various momenta are shown in Figs. 3(b)–3(d). In between **M** and the Fermi crossing [Fig. 3(b)], the upper part of the low temperature spectrum is overlaid with the normal state spectrum, which is a sign of gap opening. This is clearly illustrated by the weight suppression in the CDW state of the "recovered spectra" (on the right), where the thermal broadening effects are compensated by dividing the resolution convoluted Fermi-Dirac distribution function. Normalized by the corresponding integrated "recovered" spectral weight over $[E_F - 0.1\ eV, E_F]$ in the normal state, the spectral weight suppression ratio map [lower half of Fig. 3(a)] resembles the gap map, as they both characterize the global distribution of the gap. In Fig. 3(c), for the spectrum at the inner Γ Fermi pocket, no sign of a gap opening is observed, consistent with previous studies [7,8]. Figure 3(d) illustrates that a gap of 19 meV is observed at the saddle point of the band calculation. An alternative mechanism was proposed for $2H$-TMD's involving the scattering between saddle points, which would cause a singularity in density of states, and thus an anomaly in the dielectric response function [20]. The gap near this point has been reported before [21], but the distance between these points do not match the CDW ordering wave vectors [22,23]. In the current gap map, no singularity is observed for this momentum.

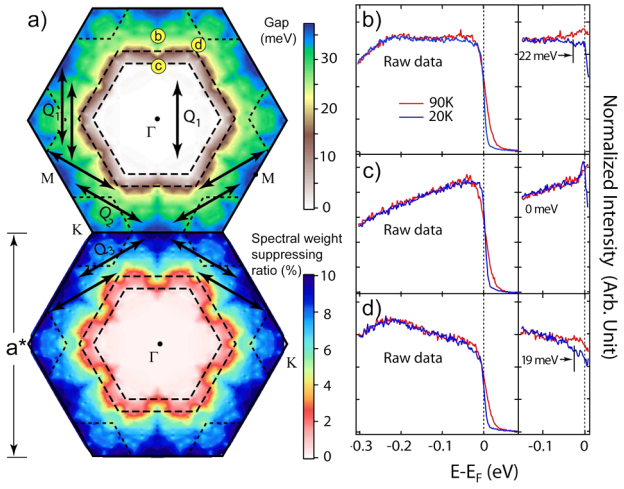

FIG. 3 (color online). (a) The false color plots of the CDW gap (upper half), and the spectral weight suppression ratio map (lower half, see text for explanation) in the first Brillouin zone of CDW$^{65\ K}$, where the dashed lines indicate the Fermi surfaces. States in the gapped region could be connected by the CDW wave vectors, $\mathbf{Q}_i$ $(i = 1, 2, 3)$, as indicated by the double-headed arrows. (b)–(d) comparison of the typical spectra in normal and CDW states at various momenta marked by the circled letters in (a). The spectra on the right have been divided by resolution convoluted Fermi-Dirac functions at corresponding temperatures.

The CDW in TMD's is accompanied by structural transitions [5,6]; therefore electron-phonon interactions are also important. Since the low energy electronic structure of $2H$-Na_xTaS_2 is dominated by the Ta $5d$ electrons [13], among which Coulomb interactions are usually weak, the broad ARPES line shape would suggest strong electron-phonon interactions. A kink in the dispersion corresponding to the phonon energy scale was found for $2H$-Na_xTaS_2 (not shown here) as in other $2H$-TMD compounds [24]. In this context, the anisotropic gap distribution might be attributed to the anisotropy of electron-phonon couplings [25,26], and states in the ungapped region simply may not couple with the relevant phonons. One critical requirement, i.e., states in different gapped regions need to be coupled by phonons and/or charge fluctuations with the CDW wave vectors, can now be fulfilled in the gap map, as illustrated by the arrows in Fig. 3(a). $\mathbf{Q}_i = \mathbf{a}_i^*/3$ $(i = 1, 2, 3)$ here are the CDW wave vectors, $\mathbf{a}_i^*$'s being the reciprocal lattice vectors along the three Γ-**M** directions. This also explains why the size of the Fermi surfaces can vary significantly for different $2H$-TMD systems, with nearly system-independent CDW ordering wave vectors [22,23,27]. On the other hand, charge fluctuations with indefinite wave vectors are allowed over the Fermi patch. To address why $\mathbf{Q}_i$'s are favored, the joint density of states,

$$C(\vec{q}, \omega) \equiv \int A(\vec{k}, \omega)A(\vec{k}+\vec{q}, \omega)d\vec{k},$$

where $A(\vec{k}, \omega)$ is the spectral function, is calculated, as it describes the phase space for scattering of electrons from the state at $\vec{k}$ to the state at $\vec{k}+\vec{q}$ by certain modes with wave vector $\vec{q}$. Therefore, one would expect that it peaks at the ordering wave vector for $\omega = 0$ near the phase transition of static order. This autocorrelation of ARPES spectra has been demonstrated to give a reasonable count for the charge modulations observed by STM in cuprate superconductors [28,29]. Since the states in the gapped Fermi patch are responsible for the CDW here, autocorrelation analysis is conducted in the normal state to study the CDW instabilities of CDW$^{65\ K}$ over regions that would be

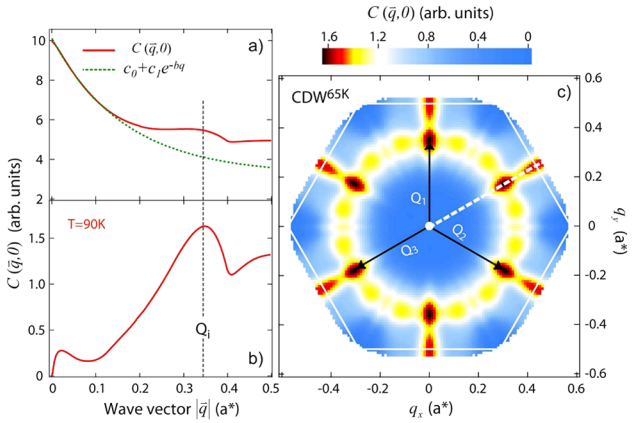

FIG. 4 (color online). (a) Autocorrelation of the ARPES intensity at E_F in the normal state of CDW$^{65\ K}$ for wave vector along the Γ-**M** direction. The dashed line is an exponential decay plus a constant, which is deducted in (b) to highlight the structure. (c) The partial autocorrelation in the 2D momentum transfer space obtained in the same way as in (b). Repeated zone scheme is taken in the integration, and thus $C(\vec{q}, 0)$ is symmetric with respect to the boundaries (white hexagon).

gapped below T_{CDW}. The resulting $C(\vec{q}, 0)$ is shown in Fig. 4(a) for $\vec{q}$ along the Γ-**M** direction, which mainly consists of a component at $\vec{q} = 0$ that exponentially decays, and several features in Fig. 4(b), where a peak is clearly observed around the CDW ordering wave vector. The peak at $\vec{q} = 0$ would require coupling to very long wavelength phonons, which presumably is very weak. Consistently, a recent calculation has shown that an optical phonon branch softens significantly around $\mathbf{Q}_i$, and no sign of softening is observed at $\vec{q} = 0$ [30]. In the 2D partial $C(\vec{q}, 0)$ map (obtained after deducting the exponential decaying part and the constant background) in Fig. 4(c), although there are a few local maxima corresponding to various possible orderings, the highest peaks are those at $\mathbf{Q}_i$. Therefore, our results suggest that the electronic structure is in favor of the charge instability at $\mathbf{Q}_i$'s, and eventually the system becomes unstable to the CDW formation below T_{CDW} in collaboration with the phonons. Furthermore, it is also consistent with the positive correlation between the spectral weight near E_F and T_{CDW} in Fig. 1(i).

The competition and coexistence of CDW and superconductivity can be understood within the new framework. Recent photoemission studies have revealed that superconducting gap opens at the **K** and Γ pockets [10,25]. The CDW gap opens at a temperature higher than the superconducting transition, but it just partially suppresses the density of states around the **K** pocket and outer Γ pocket. Therefore, as observed in most 2*H*-TMD's, superconductivity is suppressed but not eliminated by the CDW.

To summarize, the Fermi-patch mechanism of CDW in 2*H*-Na_xTaS_2 is characterized by the realization of both ingredients of the CDW, energy gap and wave vector match on the Fermi patches. Unlike other CDW mechanisms based on band structure effects, it is rooted in the strong-coupling nature of its electronic structure, which provides phase space needed for CDW fluctuations. Furthermore, this mechanism would be realized not only in polaronic systems, but also in materials where strong electron correlations could cause Fermi patches, and thus CDW instabilities.

This work is supported by NSFC, MOST's 973 Projects No. 2006CB601002 and No. 2006CB921300, and STCSM. SSRL is operated by the DOE Office of Basic Energy Science under Contract No. DE-AC03-765F00515.

*dlfeng@fudan.edu.cn

[1] B. Dardel *et al.*, Phys. Rev. Lett. **67**, 3144 (1991).
[2] B. Dardel *et al.*, Europhys. Lett. **19**, 525 (1992).
[3] K. M. Shen *et al.*, Science **307**, 901 (2005).
[4] T. Nakagawa *et al.*, Phys. Rev. Lett. **86**, 854 (2001).
[5] J. A. Wilson, F. J. Di Salvo, and S. Mahajan, Adv. Phys. **24**, 117 (1975).
[6] D. E. Moncton, J. D. Axe, and F. J. Di Salvo, Phys. Rev. Lett. **34**, 734 (1975).
[7] K. Rossnagel, E. Rotenberg, H. Koh, N. V. Smith, and L. Kipp, Phys. Rev. B **72**, 121103(R) (2005).
[8] W. C. Tonjes, V. A. Greanya, R. Liu, C. G. Olson, and P. Molinie, Phys. Rev. B **63**, 235101 (2001).
[9] A. H. Castro Neto, Phys. Rev. Lett. **86**, 4382 (2001).
[10] T. Yokoya *et al.*, Science **294**, 2518 (2001).
[11] L. Fang *et al.*, Phys. Rev. B **72**, 014534 (2005).
[12] This normalization also matches the valence band at higher binding energies reasonably.
[13] G. Y. Guo and W. Y. Liang, J. Phys. C **20**, 4315 (1987).
[14] L. Kipp *et al.*, Phys. Rev. Lett. **83**, 5551 (1999).
[15] H. Ding *et al.*, Phys. Rev. Lett. **78**, 2628 (1997).
[16] N. Furukawa, T. M. Rice, and M. Salmhofer, Phys. Rev. Lett. **81**, 3195 (1998).
[17] T. Sato *et al.*, Phys. Rev. Lett. **83**, 2254 (1999); T. Yokoya, T. Kiss, A. Chainani, S. Shin, and K. Yamaya, Phys. Rev. B **71**, 140504(R) (2005).
[18] G. Grüner, *Density Waves in Solids* (Addison-Wesley Longman, Reading, MA, 1994).
[19] R. L. Barnett, A. Polkovnikov, E. Demler, W. G. Yin, and W. Ku, Phys. Rev. Lett. **96**, 026406 (2006).
[20] T. M. Rice and G. K. Scott, Phys. Rev. Lett. **35**, 120 (1975).
[21] R. Liu, C. G. Olson, W. C. Tonjes, and R. F. Frindt, Phys. Rev. Lett. **80**, 5762 (1998).
[22] Th. Straub *et al.*, Phys. Rev. Lett. **82**, 4504 (1999).
[23] K. Rossnagel *et al.*, Phys. Rev. B **64**, 235119 (2001).
[24] T. Valla *et al.*, Phys. Rev. Lett. **85**, 4759 (2000).
[25] T. Valla *et al.*, Phys. Rev. Lett. **92**, 086401 (2004).
[26] T. P. Devereaux, T. Cuk, Z.-X. Shen, and N. Nagaosa, Phys. Rev. Lett. **93**, 117004 (2004).
[27] D. E. Moncton, J. D. Axe, and F. J. Di Salvo, Phys. Rev. B **16**, 801 (1977).
[28] U. Chatterjee *et al.*, Phys. Rev. Lett. **96**, 107006 (2006).
[29] K. McElroy *et al.*, Phys. Rev. Lett. **96**, 067005 (2006).
[30] J. L. Wang and H. Q. Lin (private communication).